Evaluation of Cooling Requirements for Rotating Detonation Combustors

EVALUATION OF COOLING REQUIREMENTS FOR ROTATING DETONATION COMBUSTORS

Umberto Sandri*
DIEF - Department of Industrial Engineering of Florence
University of Florence
via S. Marta 3, 50139, Firenze, Italy
umberto.sandri@unifi.it

Shreyas Ramanagar Sridhara
DIEF - Department of Industrial Engineering of Florence
University of Florence
via S. Marta 3, 50139, Firenze, Italy
shreyas.ramanagarsridhara@unifi.it

Antonio Andreini
DIEF - Department of Industrial Engineering of Florence
University of Florence
via S. Marta 3, 50139, Firenze, Italy
antonio.andreini@unifi.it

Myles D. Bohon
Chair of Pressure Gain Combustion
Technische Universitt Berlin
Strae des 17. Juni 135, 10623 Berlin, Germany
m.bohon@tu-berlin.de

A. Picchi
DIEF - Department of Industrial Engineering of Florence
University of Florence
via S. Marta 3, 50139, Firenze, Italy
alessio.picchi@unifi.it

B. Facchini
DIEF - Department of Industrial Engineering of Florence
University of Florence
via S. Marta 3, 50139, Firenze, Italy
bruno.facchini@unifi.it

ABSTRACT

In the last decade, the Rotating Detonation Combustor (RDC) has received growing attention among the different Pressure Gain Combustion concepts due to the simplicity of the design and the potential ease of integration in gas turbines. However, *multiple technological challenges are still associated with its development. Researchers have pointed out concerns related to the heat loads determined by the high temperature and the complex flow field occurring in this kind of combustion chamber based on a small but meaningful set of experimental and numerical results. An investigation of the open literature has shown a strong sensitivity of the heat loads with multiple designs and operational parameters. The aim of this work is to provide a fundamental review of the primary drivers affecting heat load in a typical RDC in order to define basic cooling requirements for possible actual design of the combustor. Along with this, a simplified approach has been implemented for the estimation of the requirements for cold side convection cooling with respect to different heat load scenarios, shedding light on the compatibility of pure convection cooling for Rotating Detonation Combustors. Finally, the results are used to determine guidelines for the design of a cooled and efficient RDC.*

INTRODUCTION

Detonation based combustors have received growing attention in the last decades. Due to the increase in pressure occurring during the heat addition process, resulting in a smaller amount of entropy produced, this new technology determines thermodynamic cycle efficiency gains when compared to the conventional deflagrative counterparts [1]. Among the different concepts developed, Rotating Detonation Combustors (RDC) have received most of the attention from researchers worldwide. Due to the simple design without moving parts and the high frequency outlet flow, RDCs represent the most promising solution for integration in gas turbines [2].

However, many challenges are still associated with its development, and combustor cooling represents one of the most critical. The thermal load to combustors walls is driven by aerodynamic loading, surface roughness, free stream turbulence, boundary layer disturbances, hot gas temperature, pressure profiles, and periodic unsteadiness [3], and all of these flow field features are pronounced in RDC. Indeed, the flow field in such combustors is characterized by a rotating detonation wave spinning at a frequency of several kHz with deflagration occurring at the contact surface between fresh and burnt gases, an oblique shock wave attached to the top of the detonation wave spinning at its same frequency, a highly turbulent flow field, and extremely high temperatures [4]. These flow field features are clearly visible in the results provided by the same lead author and shown in Fig. 1.

For these reasons, many researchers have attempted to quantify the thermal load acting on the liner of this type of combustor by means of different approaches. The first heat flux measurements have been performed by Bykovskii and Vederniko [5] in 2009 who showed that for identical flow rate, continuous spin detonation determined thermal loads on the combustor walls similar to those usually measured in conventional types of combustors, with values of 1 MW/m^2. However, they pointed out that the character of the heating environment depends on the number of waves. In 2014 Theuerkauf et al. [6] performed heat flux measurements using a two-sided Resistance Temperature Detector (RTD) array installed in a water-cooled RDC. The RDC has been operated at ambient conditions and without outlet restrictions, determining a fresh gas pressure close to 1 *bar*. Their results clearly indicated that maximum heat flux values were identified when a steady rotating detonation was established inside the RDC and pointed out an increase in its value, with increasing mass flow and equivalence ratio.

Then, in 2016, Theuerkauf et al. [7] compared these experimental results with numerical simulation. The CFD model consists of a solver of quasi-two-dimensional, single-species, reactive Euler equations with source terms. A methodology has been implemented to dump the highest frequency unsteadiness. Their results indicated good agreement between peak values of heat flux, with experimental results laying between two standard deviations of the experimental results, identifying heat flux peaks of $25MW/m^2$. Bulk averaged values ranged between 0.5 and 2.5 MW/m^2 for the numerical results while the experimental results showed heat flux values always in the vicinity of $1MW/m^2$ along the axial direction of the RDC, confirming the results of Bykovskii and Vederniko [5] previously presented.

Further heat flux measurements with the use of heat flux gauges have been performed by Meyer et al. [8] in 2017. In this study, a twelve sensor thin film heat flux gauge array, designed to improve the durability and reliability of the instruments used by Theuerkauf et al. [7] was used to investigate the impact of different mass flow and equivalence ratios on the heat flux on the walls of an uncooled RDC. The results have shown an increase in heat flux due to increasing mass flow, and thus mass flux in the fixed channel width geometry, and of equivalence ratio. Furthermore, they have identified a steady increase in heat flux due to the increase of wave speed, independently of the mass flow rate considered. Yet the highest wave speed has been obtained for the largest mass flow and equivalence ratio considered in the study.

By means of the same experimental techniques, the following year, the same authors [9] investigated the impact of other operational parameters on the heat flux and measured average values ranging between 0.1 and 0.36 MW/m^2. The results indicated a 12% increase of heat flux as the annulus width increased from 16.3 mm to 22.5 mm, reaching its maximum value at a richer equivalence ratio. The use of an aerospike, acting as an outlet restriction and thus increasing the combustion chamber pressure, did not result in changes in the average value of heat flux, but deteremined a change in the peak axial location of the heat flux measured. The major driver for the increase in the heat flux was identified with the increase in equivalence ratio.

An investigation of the effects of the outlet restriction has also been performed the following year by Goto et al. [10]. They measured average values of 2.1 MW/m^2 and indicated an almost linear relation between the total pressure in the combustion chamber, and the measured heat flux. Heat flux measurements have also been performed by Stevens et al. [11], who measured heat flux values ranging between 0.8 and 1.4 MW/m^2 increasing with higher values of mass flux and equivalence ratio considered.

Values of heat flux provide insight into the overall thermal load associated with RDC operations. However, in order to define the cooling requirements for RDC, it is required to know a value of heat transfer coefficient between the hot gases and the liner walls, representative of both convective and radiative heat transfer, linearizing the latter, and the temperature of the hot gases in the combustor. Fewer works providing these results are available.

The first heat transfer coefficient measurements have been performed by Meyer et al. [8], who showed values of the heat transfer coefficient increasing from 0.2 to 1.4 $kW/(m^2K)$ with increasing mass flow and equivalence ratio. The measurements have been performed starting from the measured heat flux, dividing it with the temperature difference between the wall temperature and the average gas temperature across the RDC annulus. Stevens et al. [11] followed a similar approach for the measurement of the heat transfer coefficient. However, in this work, the gas temperature, instead of being measured, was assumed to be equal to the CJ temperature. This value represents the upper temperature limit for a detonation and thus underestimates the real value of heat transfer coefficient. Nevertheless, the results showed h_g values increasing from 0.4 to $0.9kW/(m^2K)$ indicating a monotonic increasing relationship between the detonation wave velocity and the measured heat transfer coefficient.

Table 1: Summary of the results found in literature

Author	$h_{g,min}$ $[W/(m^2K)]$	$h_{g,max}$ $[W/(m^2K)]$	q_{min} $[MW/(m^2)]$	q_{max} $[MW/(m^2)]$	Notes
Bykovskii et al. [5] EXP	-	-	-	1	No outlet restriction $P_b = P_{amb}$
Meyer et al. [8] EXP	200	1400	0.2	0.35	q_{min} : $minER = 0.7$, $minJ_g$, $minWS$ q_{max} : $maxER = 0.7$, $maxJ_g$, $maxWS$ $P_b = P_{amb}$
Meyer et al. [9] EXP	-	-	0.10	0.36	q_{min} : $minER = 0.65$ q_{max} : $maxER = 1.15$, $maxAW$ $P_b = P_{amb}$
Stevens et al. [11] EXP	400	900	0.8	1.4	q_{min} : $minWS$, $minER$, $minAW$ q_{max} : $maxWS$, $maxER$, $maxAW$ $P_b = P_{amb}$
Stevens et al. [12] EXP	200	1000	0.4	1.6	$P_b = P_{amb}$
Goto et al. [10] EXP	-	-	1	5	q_{min} : $minJ_g$, $P_{0,cc} = 1bar$ q_{max} : $maxJ_g$, $P_{0,cc} = 15bar$
Braun et al. [13] NUM	900	7000	~ 1	$\sim$10	1D det + MOC + Correlations $1bar < P_{fg} < 20bar$
Nassini et al. [14] NUM	-	2640	-	1.7	LES + Wall Function $P_{plenum} \sim 12bar$, $P_{fg} \sim 1.5bar$

Numerical results have also contributed to the definition of the thermal load in RDC combustors. Braun et al. [13] developed a reduced order model for the definition of the RDC flow field as a function of prescribed initial pressure and temperature of the unburnt gas mixture. Then, considering the boundary layer integral method and dedicated correlations, the heat flux and heat transfer coefficient have been calculated. This study represents the first one in which elevated pressures were considered. The results have shown a strong sensitivity of the initial pressure on the heat flux, calculating average values of heat transfer coefficient up to 7 $kW/(m^2K)$ when an initial fresh gas pressure of 20 bar was considered.

Finally, heat flux and heat transfer coefficient values have been calculated from the LES simulation by means of wall function, by Nassini et al. [4] [14]. The simulated combustor is representative, both in terms of geometry and of operating condition, of the test rig developed at the TU Berlin, described in detail by Bach et al. [15]. The test rig is operated with air supplied by a plenum pressurized at ~ 12 bar. However, the combustion chamber is exposed to the environment at atmospheric conditions and high pressure losses occur over the injection scheme and the fresh gas pressure is around 1.5 bar, as indicated by the LES simulations. The results indicated an average value of the heat transfer coefficient on the outer wall of the RDC equal to $2.64kW/(m^2K)$. Heat flux time averaged profiles along the RDC axial direction have been provided only by a few of the works presented in the introduction and the results have been summarized in Fig. 2.

The results presented show some common trends. Generally, Braun et al. [13] and Theuerkauf et al. [7] showed lower values of heat flux at low axial positions. This is assumed to be caused by the cooling effects of the unburnt gases. While being extremely meaningful for a comparative analysis of the influence of different operating parameters on the heat flux, these results don't provide sufficient information to define the boundary conditions for the design of a cooling system for RDC.
Indeed, review of the literature summarized in Table 1, indicates that a strong sparsity in the results exists among both measured and calculated values of heat flux and heat transfer coefficients due to the different design and operating conditions considered in the different experimental test rigs and numerical simulations. This occurs because RDCs are still at a relatively low technology readiness level. An optimal configuration in terms of design and operating parameters, such as limits in the annulus width, inner and outer liner diameter, injection scheme, fuel used, mass flux required, fresh gas pressure, have not been defined yet. All these variables are coupled and affect the flow field features of the RDC and thus the thermal load.

Furthermore, strong heat loads don't represent the only challenge associated with the cooling of RDC combustors. Conventional combustors are usually implemented with film cooling technologies, relying on the pressure gradient between the burning gases and the air discharged by the compressor. In RDC, the pressure gain occurring during the combustion process would partially impede this approach, unless further compression is provided to the coolant air by a booster compressor, as conceptualized by Stathopoulos et al. [16] for the cooling of the first turbine cascade. A modified version of the layout, adapted from [16] with the integration of combustor cooling, is shown in Fig. 3.

Additionally, if no booster compressor is integrated, structural challenges could be associated with the negative pressure gradient across the liner walls, especially in the lower combustor part, associated with the detonation region. In this context, this paper attempts to provide an initial path toward the development of cooling solutions for the RDC. As an output of the literature review, ranges of realistic thermal loads are defined considering the application of a RDC in a real-scale engine. A fast evaluation procedure is implemented, allowing an assessment of the required heat transfer capabilities for a cold side convection cooling solution identifying the amount of required cooling air and associated pressure losses. Limits for the implementation of forced convection cooling are defined with respect to the investigated variable space and conclusions and suggestions for future investigations are provided.

Input Required For Cooling System Design

The results presented in the introduction characterized the heat load environment of RDC by means of numerical and experimental activities. One of the most characteristic aspect of RDC consists of the strong unsteadiness associated with high frequency rational speed of the detonation wave. For this reason, researchers measured heat flux and convective heat transfer coefficient, presenting both time resolved and average values. This section investigates the effect of the dynamic component of the thermal load on the temperature profile within the liner, investigating its penetration depth. It is possible to investigate this behavior by modeling the heat transfer across the RDC liner with the equation for the heat diffusion in cylindrical coordinates as presented in Eq. 1.

$$
\begin{aligned}
&\frac{1}{r}\frac{\partial}{\partial r}\left(rk\frac{\partial T}{\partial r}\right) = \rho c\frac{\partial T}{\partial t} \\
BC: \quad &@x = 0 \quad -k\frac{\partial T}{\partial r} = h_g(T_g(t) - T(0,t)) \\
&T_g(t) = T_{g,mean} + \Delta T cos(\omega t) \\
&@x = L \quad -k\frac{\partial T}{\partial r} = h_c(T(L,t) - T_c) \\
IC: \quad &@t = 0 \quad T(r,0) = T_{m,initial}
\end{aligned}
\tag{1}
$$

The problem is associated with a uniform initial temperature and two Neumann boundary conditions are imposed on the two ends of the 1D domain. An analytical solution doesn't exist for this equation, however, it is possible to take advantage of models describing the penetration depth of the temperature oscillation. According to Salazar [17], if the product between the $\omega = 2\pi f$ and the material thermal relaxation time τ is much smaller than 1, then, the penetration depth μ can be defined as $\sqrt{2\alpha/\omega}$. In this equation, α, the material thermal diffusivity, is defined as $\alpha = k/(\rho c)$ with k, ρ, and c being the thermal conductivity, the density and the specific heat of the material respectively. In the present study, a general nickel-base alloy commonly used for liner construction is considered and the material properties are defined in Table 2.

Locally, inside a RDC, the frequency of the peaks in the gas temperature correspond to the frequency of rotation of the detonation wave. The frequency of the detonation depends on multiple design and operational parameters such as the size of the combustor and the equivalence ratio of the gas mixture; however it has been reported by many authors to be in the order of several kHz [6] [14]. The

Table 2: Liner Material properties

Material Property	Value	Reference
Density ρ	8370 kg/m^3	[18]
Thermal Conductivity k	26 $W/(m^2K)$	[19]
Heat Capacity c	461 $J/(kgK)$	[18]
Temperature limit	1100 K	[19]

relaxation time of metals is reported to range between 10^{-9} and 10^{-12} seconds [17]. Applying the calculation to the heat load scenario occurring in an RDC, even considering a very low frequency of 1 kHz which is well below common values reported in literature [11], it was possible to measure a penetration depth of $\sim 50\ \mu m$. This value is two orders of magnitude lower than the typical thickness of a liner, indicating that the material thickness dampens out the heat load fluctuations before the cold side is reached. Thus, for the definition of the cooling requirements obtained with the one dimensional approach defined below, the dynamic component of the thermal load can be neglected. This calculation is also extended to other materials commonly used in combustion laboratory and the results relative to the calculated penetration depths, leading to analogous conclusions, are presented in Table 3.

Table 3: Temperature fluctuations penetration depth considering different materials

Material	Themal Diffusivity $\alpha\,[m^2/s]$	Penetration Depth $\mu\,[\mu m]$
Stainless Stell AISI316L	$4.0 \cdot 10^{-6}$	35
Bronze Beryllium Copper UNS C17200	$0.37 \cdot 10^{-6}$	109
Brass UNS C28000	$0.39 \cdot 10^{-6}$	111

Fast evaluation procedure

Due to the complex flowfield occurring inside an RDC, convection cooling on the cold side of the liner could represent a solution for maintaining the liner walls within prescribed temperature limits and avoiding the injection of coolant flow inside the combustion chamber. However, convection cooling can require large amounts of coolant flow and associated pressure losses, which result in detrimental effects on the gas turbine cycle efficiency. For this reason, in order to investigate the impact of the wide range of thermal loads on the cooling requirements it is necessary to develop a fast evaluation procedure for its assessment. Figure 4 shows in a schematic way how the input variables are combined to define the cooling requirements.

For this purpose, the concept of cooling effectiveness is introduced. The cooling effectiveness is defined as in Eq. 2,

$$\Phi = \frac{T_g - T_{m,g}}{T_g - T_{c,in}} \tag{2}$$

where T_g represents the temperature of the gas, $T_{m,g}$ the temperature of the metal, in this case of the liner, on the gas side, and $T_{c,in}$ the initial temperature of the coolant. For the calculation of the required cooling effectiveness Φ_{req}, $T_{m,g}$ is always imposed to be equal to 1100 K, corresponding to the target temperature at the wall. $T_{c,in}$ is calculated as a function of the Overall Pressure Ratio (OPR) at which the considered combustors would operate, assuming a compressor isentropic efficiency $\eta_{c,is}$ equal to 0.95 and an initial air temperature of 290K. Once the required cooling effectiveness is defined, it is possible to assess the compatibility of a cooling scheme with a certain heat load by comparing Φ_{req} with the cooling effectiveness achievable Φ_{ach} by the system. The RDC consists of an annular combustion chamber. Considering the outer liner, the cooling channel consist of another annulus, with inner and outer boundaries represented by the combustor cold side outer liner wall and a larger cylinder respectively. Analogous considerations can also be made for the inner RDC liner. The achievable cooling effectiveness can thus be expressed as a function of two other parameters, namely the Heat Load Parameter (HLP) and the cooling system thermal efficiency η_{th} expressed as follows:

$$HLP = \frac{\dot{m}_c c_{p,c}}{A_g h_g} \tag{3}$$

$$\eta_{th} = 1 - exp\left(\frac{-1}{\dot{m}_c C_p \left(\frac{1}{A_c h_c} + \frac{ln(R/r)}{2\pi L k_m}\right)}\right) \tag{4}$$

The HLP represents the ratio between the capability of the coolant of absorbing heat, defined as the product between the coolant mass flow $\dot{m}_c$ and the heat capacity of the coolant $c_{p,c}$, and the heat load imposed on the part, expressed as the product between the area exposed to the hot gases A_g and the average heat transfer coefficient on the gas side h_g. The thermal efficiency η_{th} represents the ratio of the actual coolant temperature increase over the maximum coolant temperature increase achievable. It depends on the coolant mass flow, its heat capacity and the thermal resistance between the gas side liner wall and the coolant flow, expressed as the sum of a convective and a conductive thermal resistance as described in Eq. 4, adapted from the expression reported by Downs and Landis [20] to account for the curvature of the liner. A_c represents the area contributing to the coolant cold side convection cooling, where h_c is the heat transfer coefficient describing the heat transfer between the liner wall on the coolant side and the coolant itself. R and r represent the larger and smaller radius of the considered liner, and the difference corresponds to the liner thickness. L is the RDC liner length and k_m is the thermal conductivity of the liner. Based on the definition of HLP and η_{th}, it can be shown that the cooling effectiveness can be expressed as follows:

$$\Phi_{ach} = \frac{\eta_{th} HLP}{1 + \eta_{th} HLP} \tag{5}$$

In order to identify the requirements of a cooling system, the achievable cooling effectiveness is parameterized as a function of the coolant mass flow $\dot{m}_c$ used, expressed as a percentage fraction of the mass flow directly participating in the combustion $\dot{m}_g$ and by means of the heat transfer performance associated with a cooling scheme, characterized by a value of Enhancement Factor $EF = Nu/Nu_0$, representing the enhancement of Nusselt number of a considered technology with respect to that of a smooth channel, with the same geometrical characteristics. The Nusselt number of the coolant, Nu_c is calculated considering both parameters, EF and $\dot{m}_c$. Nu_0 are calculated according to the well-established Dittus-Boelter correlation with a correction accounting for the high temperature difference between the coolant and cooled wall, defined as in Eq. 6, according to [21].

$$Nu = (0.023 Re_c^{0.8} Pr_c^{0.4}) \cdot \left(\frac{\mu(T_c)}{\mu(T_{m,c})} \right)^{0.14} \qquad Re_c = \frac{\frac{\dot{m}_c D_h}{A_{CC}}}{\mu(T_c)} \tag{6}$$

While the Reynolds number is defined as in the equation above, the Prandtl number is kept constant in this investigation, with a value of 0.71. This assumption is justified by the small variations in the range of considered coolant temperatures and the negligible sensitivity of its value on the output of the calculation. The equation above is validated for Reynolds numbers above 10^4, $L/D > 10$ and Prandtl numbers above 0.7 [21]. A_{CC} is the cross sectional area of the cooling channel and it is calculated as a function of the considered liner wall diameter and the coolant channel width. In this way, for a selected thermal load defined by a prescribed value of gas temperature T_g and a heat transfer coefficient between the gas and the liner walls h_g downstream of the selection of geometrical characteristics of the liner and of the coolant channel and of a reference OPR, it is possible to identify a required cooling effectiveness and the set of combinations of EF and $\dot{m}_c$ that allow to achieve it.

Furthermore, for the characterization of a cooling system, it is interesting to calculate the pressure losses associated with a certain combination of EF and $\dot{m}_c$ allowing the achievable cooling effectiveness to be equal to the required cooling effectiveness. The Pressure

Losses are defined according to the following equation:

$$Pressure\,Losses = \frac{\Delta P}{OPR} \qquad \Delta P = \frac{f \rho L v^2}{2D_h} \tag{7}$$

The value of f is obtained considering a certain value of f/f_0 and multiplying it with a value of f_0, calculated according to the well established Colebrook correlation for smooth tubes, defined as in Eq. 8, valid for Reynolds numbers between $3 \cdot 10^3$ and $2 \cdot 10^8$, according to [22].

$$f_0 = [0.79 lnRe_c - 1.64]^{-2} \tag{8}$$

In the procedure, a certain value of f/f_0 is associated with any value of Nu/Nu_0 considering a level of Efficiency Index (EI) as described below. In general, the relation between Nu/Nu_0 and f/f_0 is strictly related to a specific geometry selection and the considered Reynolds number of the coolant flow. However, in this case a strategy is implemented to maintain a level of generality and without considering the specific aspects mentioned above. The most common way to characterize the performance of a convection cooling scheme is to scale the Nusselt Number and the friction factor considering an Efficiency Index (EI) defined as follows:

$$EI = \frac{Nu/Nu_0}{(f/f_0)^{1/3}} \tag{9}$$

To define a value of EI to be considered in the present study, the result provided by Ligrani et al. [23] are considered. In this study, the performance of a wide range of cooling schemes over a wide range of Reynolds numbers have been measured and the results plotted in a chart relating Nu/Nu_0 and f/f_0 . Figure 5 is adapted from their paper, plotting on top of it lines of iso-EI, with values increasing from 0.9 to 1.5. Those lines span over the whole variable space represented by the results identified in literature. In this way, it is possible to associated a value of f/f_0 to every value of Nu/Nu_0 allowing the calculation of the pressure losses.

1 Input Variable Definition

To assess the cooling requirements, it is necessary to define the geometrical characteristics and the heat load environment associated with RDC operations.

1.1 Geometrical Variables Definition

The objective of this study is to assess the cooling requirements for RDC for implementation on a real engine. To begin, we start considering a reference engine assuming to substitute cannular combustors with RDCs. It has been shown that the efficiency gain of this type of combustor is higher when operated at a low overall pressure ratio [16, 24]. For this reason, a low OPR heavy duty gas turbine is considered. The main characteristics of the considered gas turbine are summarized in Table 4.

Table 4: Characteristics of selected reference Gas Turbine

Parameter	**Value**
Power Output	2 $[MW]$
Gross Efficiency	0.25 $[-]$
Thermal Power Input	8 $[MW]$
LHV H_2	120 $[MJ/kg]$
Number of can combustors	4
Overall Pressure Ratio	7 $[-]$

For the sake of clarity, in this simplified approach it is assumed that the RDC wouldn't determine a pressure gain, thus, an RDC-retrofitted version of the engine would determine the same power output if operated at OPR equal to 7 and providing the same thermal power input, as suggested by Stathopoulos et al. [16]. In this study, hydrogen is considered as fuel for two reasons:

Hydrogen has been widely used in RDC tests because of its high reactivity and thus ease in achieving a detonation.

Hydrogen is considered one of the most promising solution for the development of gas turbines in the early future.

Thus, considering hydrogen combustion at a stoichiometric condition for the RDC, it is possible to calculate the gas mass flow (hydrogen and air) through each combustors. The results indicate a gas mass flow = 0.6 kg/s, which roughly corresponds to the mass flow supplied to the TU Berlin RDC leading to successful operations as indicated by Bach et al. [25]. For this reason, the geometrical characteristics of the TU Berlin RDC, associated to a mass flow of gas = 0.6 kg/s and an OPR = 7 are considered the baseline configuration. However, the experimental facility isn't yet equipped with a cooling system and presents thick liner walls for safety reasons. According to Lefevbre [19], combustor liners typically present a thickness of 1.2 mm. In the present study, the conservative choice of a liner thickness of 3 mm is made to guarantee structural stability under the effect of the high frequency detonation wave. The coolant channel width, CCW, is selected equal to 4 mm, allowing to maintain the flow below Mach number of 0.3, in the whole investigated variable space, avoiding compressibility effects. A summary of the geometrical features is provided in Table 5. It is also interesting to investigate the impact of considering a larger power output gas turbine on the cooling requirements and thus a larger combustor is also considered. For the purpose of geometrically scaling the RDC, it is chosen to maintain the same annulus width and the same gas mass flux considered in

Table 5: Geometrical characteristics of the baseline geometry, adapted from Bach et al. [15]

Part	**Size**
Liner Length	110 mm
Liner Outer Diameter	90 mm
Liner Inner Diameter	74.8 mm
Annulus Width	7.6 mm
Liner Thickness	3 mm
Coolant Channel Width	4 mm

the baseline configuration, allowing to define up-scaled versions to investigate.

1.2 Thermal Load Variable Definition

As highlighted in the introduction, there is a wide sparsity in the results relative to the heat loads in RDC. Nevertheless, some trends have been identified. It has been shown that the heat load generally increases with increasing mass flux, increasing equivalence ratio, and increasing pressure. However, Meyer et al. [8] and Stevens et al. [11], showed an increase in heat flux due to an increase in the speed of the detonation wave, changing without identifying a relation with variations of mass flow and equivalence ratio. Finally, Bach et al. [25] has shown in detail that the detonation mode itself also varies as a result of a variation in mass flux, outlet restriction, and injection scheme. All these results allow to define trends but are not sufficient to generalize the results in terms of heat load for a selected reference design associated with certain reference operating conditions. Furthermore, the optimal design and operating conditions for RDC implementation in gas turbines are still undefined. For these reasons, in the present study, the heat load will be characterized by an extended combination of gas temperatures and heat transfer coefficients on the gas side, and the impact on cooling requirements will be investigated. The gas temperature is mostly driven by the OPR, due to the increase in temperature linked to compression and the joint impact with the equivalence ratio on the adiabatic flame temperature. For this purpose, the gas temperature is selected to span from 1800 to $2500K$. The convective heat transfer coefficient resulted to be mostly driven by the detonation mode and detonation speed in the RDC. The speed can be considered equal to the ideal Chapman-Jouget speed, which is a function of the static pressure, the temperature and the equivalence ratio of the fresh unburnt gases while the detonation mode is determined by a wide combination of design and operational parameters [15]. For this reason h_g is chosen to span over the wide range from 500 to $4000W/(m^2K)$. A detailed analysis will also be performed on the T_g and h_g calculated by Nassini [14].

2 Results and Discussion

2.1 Specified Heat Load

Firstly, the results relative to the outer liner of the baseline geometry defined above, considering an OPR = 7 and the thermal load calculated by Nassini [14] are considered. This condition represents the baseline scenario in the present paper. The calculated average T_g and h_g on the outer liner of the RDC are equal to 1718 K and 2640 $W/(m^2K)$ respectively. The required cooling effectiveness is thus equal to 0.51. Using the previously described tool, it has been possible to generate the maps shown in Fig 6, in which the achievable cooling effectiveness is plotted as a function of the parameters Nu/Nu_0 and $\dot{m}_c = \%\dot{m}_g$. The line representing the points where Φ_{ach} is equal to the Φ_{req} is highlighted in blue.

Figure 6 shows that the required cooling effectiveness can be achieved for a range of fraction of mass flow of gas used as coolant and cooling system performance Nu/Nu_0. A minimum mass flow equal to the 15% of the mass flow of gas is considered to allow Eq. 6 and Eq. 8 to be applied within their validity range for all the considered configuration. Requirements in terms of geometry and Prandtl number are also respected, guaranteeing reliability of the results obtained. In order to choose the optimal solution, it is necessary to investigate the associated pressure losses. Here, the associated pressure losses are calculated considering the most optimistic performance index, EI = 1.5. The results are shown in Fig. 7, where, on top of the pressure losses map, in white is plotted the line indicating the conditions where Φ_{ach} is equal to the Φ_{req}.

It is clear, that for the considered heat load, thermal management with cold side convection cooling represents a great challenge. A low Nu/Nu_0 geometry would require pressure losses slightly below 10% but would require an amount of coolant flow equal to the mass flow of gas participating in the combustion process. Moving along the y-axis toward higher EF geometries, the amount of required coolant mass flow is reduced but the associated pressure losses would increase, until the configuration characterized by an EF = 6, coolant mass flow equal to the 60% of $\dot{m}_g$ and pressure losses approaching 15%. Stathopoulos et al. [16] performed a cycle thermodynamic analysis of gas turbines equipped with pressure gain combustion combustor and showed that for an engine operating at an OPR = 10, devoting 16% of the mass flow of gas to the cooling of the first three turbine cascades it was still possible to obtain an efficiency gain with respect to the baseline gas turbine cycle. However, the amount of coolant mass flow identified here is much greater, and the associated pressure losses are well above the pressure losses usually considered acceptable for turbine cooling, identifying the limits of cold side convection cooling for RDC combustors, even considering an optimistic value of EI. A common approach considered for the reduction of cooling requirements is represented by the use of Thermal Barrier Coating (TBC). It consists of a thin layer of ceramic material applied to the hot side of the liner used to protect the liner from the high temperature environment. Its impact on the considered baseline configuration can be assessed modifying the HLP presented in Eq. 3, in order to take into account of the thermal resistance determined by the TBC, leading to the following expression:

$$HLP_{TBC} = \dot{m}_c c_{p,c} \left(\frac{1}{A_g h_g} + \frac{ln(R_{TBC}/r_{TBC})}{2\pi L k_{TBC}} \right) \tag{10}$$

Considering a typical TBC thickness $t_{TBC} = 0.25mm$ and thermal conductivity $k_{TBC} = 0.9W/(m^2K)$ as selected by Downs and Landis [20], Fig. 8 shows how the requirements in terms of Nu/Nu_0 and $\dot{m}_c = \%\dot{m}_g$ for obtaining the unvaried Φ_{req} are reduced with the implementation of this technology.

It should however be kept into consideration that there is no literature available about the performance of TBC in the detonative RDC environment characterized by high frequency temperature and pressure fluctuations. Difficult challenges are expected to arise relative to the mechanical resistance of this ceramic material for prolonged operations.

2.2 Generalized Thermal Load

Since a variety of thermal loads in RDC and strong variations associated with varying design and operational parameters has been identified, the investigation is continued spanning over a wide combination of thermal loads, as described in subsection 1.2. For a considered configuration, characterized by its geometrical features, OPR and $\dot{m}_c$, it is possible to span over the whole test matrix of thermal load inputs. Then, for every combination of h_g and T_g it is possible to identify the pressure losses required by the cooling system to determine a $\Phi_{ach} = \Phi_{req}$.

These results, shown in Fig. 9, are relative to the baseline geometry, OPR = 7, $\dot{m}_c = 50\%\dot{m}_g = 0.3kg/s$ and considering an EI = 1.5 for the calculation of the pressure drop. The map shown indicates that the capability of forced convection cooling systems for RDC are mostly limited by the heat transfer coefficient on the gas side. Figure 9 shows that considering a mass flow of coolant equivalent to half of the mass flow participating in the main combustion process, the possibility of performing cold side convection cooling is limited to a h_g value of 1950 $W/(m^2K)$ considering a gas temperature of 1800K, with this limit decreasing to $\sim$ 1000 $W/(m^2K)$ considering a gas temperature of 2500K. Along the line describing the limits within which exists a compatibility of convection cooling with specified thermal loads, the associated pressure drop describes an isoline corresponding to pressure losses equivalent to $\sim$ the 8.5%.

In order to investigate the impact of a higher fraction of mass flow used for cooling, it is possible to repeat the operation several times and retain in the results only the isoline of pressure losses describing the limiting conditions selected considering the 95% of the maximum $\Delta P/P$ identified in the performance maps presented in Fig. 9 for every considered $\dot{m}_c = \%\dot{m}_g$.

These results are shown in Fig. 10 where for every fraction of gas mass flow considered for cooling, characterized by different colors, for both $OPR = 7$ and $OPR = 14$, the set of points describing the limits of maximum h_g and T_g within which cold side convection cooling is compatible with the thermal load is shown, and the pressure losses associated with those conditions are written along the lines.

It is visible that as greater amounts of coolant are considered, the limits within which cold side convection cooling is possible are extended. Considering the case at $OPR = 7$ it is possible to maintain the liner within the prescribed temperature limit even with h_g up to $\sim 2900 W/(m^2K)$ considering a gas temperature of 1800 K. However, the maximum allowable h_g drastically decreases to $\sim$ 1400 $W/(m^2K)$ for gas temperatures of 2500 K. Furthermore, as the limits are extended, thanks to the use of greater amounts of coolant mass flow, the associated losses also increase, determining the further reduction in thermodynamic cycle efficiency.

Considering the higher OPR case, the range of h_g and T_g is decreased, as well as the associated pressure losses. This behavior is mostly driven by two system changes associated with an increase in OPR

The coolant gas temperature increases, thus determining a higher value of required cooling effectiveness.

Since the calculated pressure drop is normalized with the inlet pressure (see Eq. 7), operating at higher OPR determines a lower relative pressure losses for comparable absolute values of pressure losses ΔP.

For these reasons, for a specified thermal load, increasing the pressure determines a progressive increase in the minimum mass flow and a progressive decrease in the relative pressure losses required to maintain the liner within the prescribed temperature limit for a given combination of T_g and h_g. As a result, when a higher OPR is considered, the coolability limits defined in terms of h_g and T_g are reduced.

Further cycle analysis would be required to define the impact of those results on the overall cycle efficiency. It has been shown that increasing the OPR reduces the pressure losses required for cooling. However, this beneficial effect is degraded by the higher amount of coolant flow required and by the reduction of cycle efficiency gains associated with this PGC technology, determined by operations at higher OPR [16, 24]. All these aspects must be taken into consideration for the definition of an optimal design.

Finally, it is important to investigate the impact of considering a larger combustor on the cooling requirements. An upscaled RDC is defined considering the scaling approach previously described in section 1.1 selecting a mass flow 5 times larger than the baseline configuration. The same approach considered before is implemented relative to this new configuration and the results are presented in Fig. 11.

Generally, increasing the size of the combustors determines an increase in the surface exposed to the thermal load and in the mass flow of gases, effects which respectively have a decreasing and increasing impact on the heat load parameter. However, due to the scaling approach followed, an overall increment in heat load parameter is identified. Furthermore the increase in mass flow determines a decrease in thermal efficiency, however compensated by the increase in area exposed to the coolant gas flow, determining an overall, yet small, increase in thermal efficiency. The combination of these two effects determines a small increase on the achievable cooling effectiveness within the considered variable space. This effects determines a increase of the test matrix entrances allowing to obtain an achievable cooling effectiveness equal to the required one, thus increasing the coolability limits for RDC. The effects of considering higher OPR are the same which have been previously described for the baseline size case study. Thus, overall, considering smaller RDC and operating at higher OPR, reduces the limits within which a cold side convection cooled combustor can be developed. Furthermore, it is important to realize that all of the results presented above are relative to the cooling requirements on the outer liner alone. If also the inner liner would be considered, the associated pressure drop would be comparable, but the amount of mass flow required would approximately double. However, concepts of hollow RDC, without the inner liner have been investigated [26] [27] and could contribute to maintaining the cooling requirements within acceptable limits. Finally, in the present work, the results are obtained following a conservative approach and selecting a metal temperature limit of 1100K. Nonetheless, high temperature materials for gas turbine and RDC application, such as C/SiC composites [28], are being investigated and could play a fundamental role in the the reduction of Φ_{req} and thus of the cooling requirements.

3 RDC cooling alternative solutions

The results have indicated strong limitations for the use of cold side convection cooling schemes for maintaining the RDC liners within the temperature limits due to the large amounts of coolant required and the associated pressure losses. Furthermore, beyond heat transfer coefficient values of $\sim 2900\ W/(m^2K)$ no solution have been identified at all. A compatibility of these extreme heat loads with convection cooling can be achieved only if a booster compressor, equivalent to the concept introduced in Fig. 3, would be installed in the gas turbine. This component is required to re-pressurize the gases downstream of the liner cooling, allowing mixing with the burnt gases. Another option consists of using colder air for convection cooling. This concepts is referred to as cooled cooling air and has already shown promising results inc conventional gas turbines as shown by Bruening and Change et al. [29] who identified potential cycle improvements in the use of fuel as a heat sink. However, for this solution, additional weight and complexity have to be considered as potential drawbacks.

Finally, a challenging but promising solution can be represented by the implementation of a liner film cooling system. Film cooling is a method consisting of the injection of coolant air, at a temperature well below the gas temperature of the combustion chamber, through a grid of holes derived on the liner. In this way a protective film is created on the liner wall. This film reduces the gas temperature close to the liner wall, defined as T_g in the present study. A schematic representation of a film cooling scheme, integrated only in the oblique shock region of the combustor is shown in Fig. 12.

To asses the potential of a film cooled combustor the reference gas temperature of 1718 K is considered, in combination with OPR = 7 and an elevated but realistic value of film cooling adiabatic effectiveness of 0.35 [30]. In this scenario the required cooling effectiveness would drop to 0.25 and the cooling requirements would drastically reduce accordingly.

Figure 13 shows the impact on the requirements of considering a cold side convection cooling operating in parallel with an film cooling system characterized by an adiabatic effectiveness of 0.35. In this way the liner could be maintained at the prescribed temperature limit using a coolant mass flow equal to only the 17% of the gas mass flow and with associated pressure losses around the 2% representing an optimal result from a gas turbine efficiency point of view. However, this simple model doesn't consider two important aspects:

The increase in film cooling air temperature due to the heat absorption determined by its cooling action along the liner cold side before injection in the combustor;

the reduction in coolant mass flow participating in forced convection cooling due to the fraction of coolant flow used for convection cooling.

Yet, this model still provides an indication of the tremendous improvements which could be achieved as the assumption made can be justified in this preliminary investigation due to the short length of the combustor considered. Nevertheless, it must be recalled that RDC are characterized by the harsh environment described in the introduction and multiple challenges are associated with the implementation of this technology. On one side, the high pressure peaks determined by the detonation wave and of the oblique shock wave might determine gas ingestion in the coolant channel, on the other, the injection of coolant air could disturb and destabilize the detonation wave and, due to the supersonic character of the flow in RDC, determining the development of shock waves with all the detrimental effects on the gas turbine operations associated with it. The potential for such a system has been investigated numerically by Tian et al. [31] who indicated promising results for its implementation in the liner section spanned by the oblique shock. In the detonation region, coolant gas ingestion has been identified, locally limiting the effectiveness of the system. These results have been confirmed by Yu et al. [32], who numerically investigated film cooling in RDC and indicated a reduction of the gas ingestion phenomena when higher coolant mass flow rate are considered. Nevertheless, in the detonation region, the cold fresh gas injection already contributes to the reduction of the heat loads as showed by Goto et al. [33]. Yet, this effect is strongly dependant on the type of injection scheme, which already represents a challenge on its own, as it has as primary objective the sustenance of a stable rotating detonation. Thus, a promising solution for RDC cooling could be represented by a hybrid combination of cooling approaches, with the conceptual configuration depicted in Fig. 12. It consists of a cold side convection cooling scheme implemented over the whole length of the combustor. Alongside this, an injection scheme capable of maintaining a stable detonation while participating to liner cooling could contribute to the detonation wave section cooling, and film cooling in the section downstream of the detonation is introduced to reduce the required cooling effectiveness. With the co-participation of these three effects, the liner could be maintained within the temperature limit reducing the cycle efficiency losses associated with liner cooling.

4 Conclusion

This paper addressed the issue of cooling in RDC type combustors. An investigation of the literature identified increasing thermal load with increasing mass flux, operating pressure and equivalence ratio considered. However, it has been identified that the main driver increasing the thermal loads is represented by the detonation wave due to its contribution on the increase in convective heat transfer coefficient between the gases and the liner wall, whose speed is governed by multiple design and operational parameters. Considering the reference scenario selected in this study, the outer liner could be cooled with cold side convection cooling methods, however at the cost of very high pressure losses. Coolability limits have been defined for different RDC sizes, OPR, and amount of mass flow considered for cooling. The need for a booster compressor has been identified, either for a re-pressurization of the coolant air to allow mixing of the coolant gas with the main gas flow path or, following a film cooling approach, to actuate this strategy in this type of combustor presenting an adverse pressure gradient between the combustion chamber and the compressor discharge pressure during the passage of the detonation and oblique shock wave structure. Finally, relying on the reduction of required cooling effectiveness determined by film cooling and fresh gas injection, a promising cooling scheme integrating different strategies along the liner has been proposed as a potential solution. However, multiple challenges are associated for the definition of a cooling system for RDC. Complications might arise from the implementation of film cooling in the complex RDC flow field, and additional components such as booster compressor and mixer will be required. For this purpose, synergies between the design of a suitable cooling scheme and the definition of an optimal thermodynamic gas turbine cycle implementing RDC type of combustors, must be pursued. This approach will enable the definition of a reliable cooling strategy minimizing the costs in terms of efficiency losses.

Acknowledgments

This project has received funding from the European Unions Horizon 2020 research and innovation programme under the Marie Skodowska-Curie grant agreement No 956803

NOMENCLATURE

Roman letters

c Heat capacity [J kg^{-1} K^{-1}]

f frequency [Hz]

h Heat transfer coefficient [W m^{-2} K^{-1}]

k Thermal conductivity [W m^{-1} K^{-1}]

$\dot{m}$ Mass flow $[kg\, s^{-1}]$

P pressure[bar]

q Heat flux [W m^{-2}]

r radius / inner radius

R outer radius

Acronyms

AW Annulus width[mm]

CCW Coolant Channel Width[mm]

ER Equivalence Ratio [-]

OPR Overall Pressure Ratio[-]

WS Wave speed $[ms^{-1}]$

Greek letters

α Thermal diffusivity [m^2 s^{-1}]

η Efficiency [-]

ν Kinematic viscosity [m^2 s^{-1}]

ρ Density [kg m$^-$3]

Φ Cooling Effectiveness [-]

Dimensionless groups

f friction factor [-]

Nu Nusselt number [-]

Pr Prandtl number [-]

Re Reynolds number [-]

Superscripts and subscripts

ad adiabatic

b back

c coolant air/ compressor

fg fresh (unburnt) gas

g burnt gas / combustion side

is isentropic

m metal

p at constant pressure

req required

th thermal

th achievable

0 relative to a smooth channel / total condition

References

[1] Wolański, P., 2015. "Application of the continuous rotating detonation to gas turbine". *Applied Mechanics and Materials,* ***782***, Aug., pp. 3–12.

[2] Anand, V., and Gutmark, E., 2019. "Rotating detonation combustors and their similarities to rocket instabilities". *Progress in Energy and Combustion Science,* ***73***, July, pp. 182–234.

[3] Bunker, R. S., 2017. "Evolution of turbine cooling". In Volume 1: Aircraft Engine Fans and Blowers Marine Honors and Awards, American Society of Mechanical Engineers.

[4] Nassini, P. C., Andreini, A., and Bohon, M. D., 2022. "Propulsive performance and heating environment of rotating detonation engine with various nozzles". *Combustion and Flame*.

[5] Bykovskii, F. A., and Vedernikov, E. F., 2009. "Heat fluxes to combustor walls during continuous spin detonation of fuel-air mixtures". *Combustion, Explosion, and Shock Waves,* ***45***(1), Jan., pp. 70–77.

[6] Theuerkauf, S. W., Schauer, F., Anthony, R., and Hoke, J., 2014. "Average and instantaneous heat release to the walls of an RDE". In 52nd Aerospace Sciences Meeting, American Institute of Aeronautics and Astronautics.

[7] Theuerkauf, S. W., Schauer, F., Anthony, R. J., Paxson, D. E., Stevens, C. A., and Hoke, J., 2016. "Comparison of simulated and

measured instantaneous heat flux in a rotating detonation engine". In 54th AIAA Aerospace Sciences Meeting, American Institute of Aeronautics and Astronautics.

[8] Meyer, S. J., Polanka, M. D., Schauer, F., Anthony, R. J., Stevens, C. A., J.Hoke, and Rein, K., 2017. "Experimental characterization of heat transfer coefficients in a rotating detonation engine". In 55th AIAA Aerospace Sciences Meeting, American Institute of Aeronautics and Astronautics.

[9] Meyer, S. J., Polanka, M. D., Schauer, F. R., and Hoke, J. L., 2018. "Parameter impact on heat flux in a rotating detonation engine". In 2018 AIAA Aerospace Sciences Meeting, American Institute of Aeronautics and Astronautics.

[10] Goto, K., Nishimura, J., Kawasaki, A., K.Matsuoka, Kasahara, J., Matsuo, A., Funaki, I., Nakata, D., Uchiumi, M., and Higashino, K., 2019. "Propulsive performance and heating environment of rotating detonation engine with various nozzles". *Journal of Propulsion and Power,* ***35***(1), Jan., pp. 213–223.

[11] Stevens, C. A., Fotia, M., Hoke, J., and Schauer, F., 2018. "Quasi steady heat transfer measuments in an RDE". In 2018 AIAA Aerospace Sciences Meeting, American Institute of Aeronautics and Astronautics.

[12] Stevens, C. A., Fotia, M., Hoke, J., and Schauer, F., 2019. "An experimental comparison of the inner and outer wall heat flux in an RDE". In AIAA Scitech 2019 Forum, American Institute of Aeronautics and Astronautics.

[13] Braun, J., Sousa, J., and Paniagua, G., 2018. "Numerical assessment of the convective heat transfer in rotating detonation combustors using a reduced-order model". *Applied Sciences,* ***8***(6), May, p. 893.

[14] Nassini, P. C., 2022. "High-fidelity Numerical Investigations of a Hydrogen Rotating Detonation Combustor". PhD thesis, University of Florence.

[15] Bach, E., Stathopoulos, P., Paschereit, C. O., and Bohon, M. D., 2020. "Performance analysis of a rotating detonation combustor based on stagnation pressure measurements". *Combustion and Flame,* ***217***, July, pp. 21–36.

[16] Stathopoulos, P., 2018. "Comprehensive thermodynamic analysis of the humphrey cycle for gas turbines with pressure gain combustion". *Energies,* ***11***(12), Dec., p. 3521.

[17] Salazar, A., 2006. "Energy propagation of thermal waves". *European Journal of Physics,* ***27***(6), Sept., pp. 1349–1355.

[18] Special Metals - Home — specialmetals.com. `https://www.specialmetals.com/`. [Accessed 15-Dec-2022].

[19] Lefebvre, A. H., 1998. *GAS Turbine Combustion, Second Edition*, 2 ed. CRC Press, Boca Raton, FL, Sept.

[20] Downs, J. P., and Landis, K. K., 2009. "Turbine cooling systems design: Past, present and future". In Volume 3: Heat Transfer, Parts A and B, ASMEDC.

[21] Bergman, T. L., Lavine, A. S., Incropera, F. P., and DeWitt, D., 2011. *Fundamentals of heat and mass transfer 7E.* John Wiley & Sons, Chichester, England, Mar.

[22] Vijayan, P. K., Nayak, A. K., and Kumar, N., 2019. "Governing differential equations for natural circulation systems". In *Single-Phase, Two-Phase and Supercritical Natural Circulation Systems*. Elsevier, pp. 69–118.

[23] Ligrani, P. M., Oliveira, M. M., and Blaskovich, T., 2003. “Comparison of heat transfer augmentation techniques”. *AIAA Journal,* ***41***(3), Mar., pp. 337–362.

[24] Sousa, J., Paniagua, G., and Morata, E., 2017. “Thermodynamic analysis of a gas turbine engine with a rotating detonation combustor”. *Applied Energy,* ***195***, June, pp. 247–256.

[25] Bach, E., Paschereit, C. O., Stathopoulos, P., and Bohon, M., 2020. “RDC operation and performance with varying air injector pressure loss”. In AIAA Scitech 2020 Forum, American Institute of Aeronautics and Astronautics.

[26] Yao, S., X.Tang, and Wang, J., 2017. “Numerical study of the propulsive performance of the hollow rotating detonation engine with a laval nozzle”. *International Journal of Turbo &amp Jet-Engines,* ***34***(1), Jan.

[27] M.Tang, X., Wang, J. P., and Shao, Y. T., 2015. “Three-dimensional numerical investigations of the rotating detonation engine with a hollow combustor”. *Combustion and Flame,* ***162***(4), Apr., pp. 997–1008.

[28] Falempin, F., and Naour, B. L., 2009. “R&ampt effort on pulsed and continuous detonation wave engines”. In 16th AIAA/DLR/DGLR International Space Planes and Hypersonic Systems and Technologies Conference, American Institute of Aeronautics and Astronautics.

[29] Bruening, G. B., and Chang, W. S., 1999. “Cooled cooling air systems for turbine thermal management”. In Volume 3: Heat Transfer Electric Power Industrial and Cogeneration, American Society of Mechanical Engineers.

[30] Andreini, A., Becchi, R., Facchini, B., Picchi, A., and Peschiulli, A., 2017. “The effect of effusion holes inclination angle on the adiabatic film cooling effectiveness in a three-sector gas turbine combustor rig with a realistic swirling flow”. *International Journal of Thermal Sciences,* ***121***, Nov., pp. 75–88.

[31] Tian, J., Wang, Y., Zhang, J., and Tan, X., 2022. “Numerical investigation on flow and film cooling characteristics of coolant injection in rotating detonation combustor”. *Aerospace Science and Technology,* ***122***, Mar., p. 107379.

[32] Yu, J., Yao, S., Li, J., Huang, Y., Guo, C., and Zhang, W., 2022. “Effects of inlet and secondary flow conditions on the flow field of rotating detonation engines with film cooling”. *International Journal of Hydrogen Energy*, Dec.

[33] Goto, K., Ota, K., Kawasaki, A., Itouyama, N., Watanabe, H., Matsuoka, K., Kasahara, J., Matsuo, A., Funaki, I., and Kawashima, H., 2022. “Cylindrical rotating detonation engine with propellant injection cooling”. *Journal of Propulsion and Power,* ***38***(3), May, pp. 410–420.

FIGURES

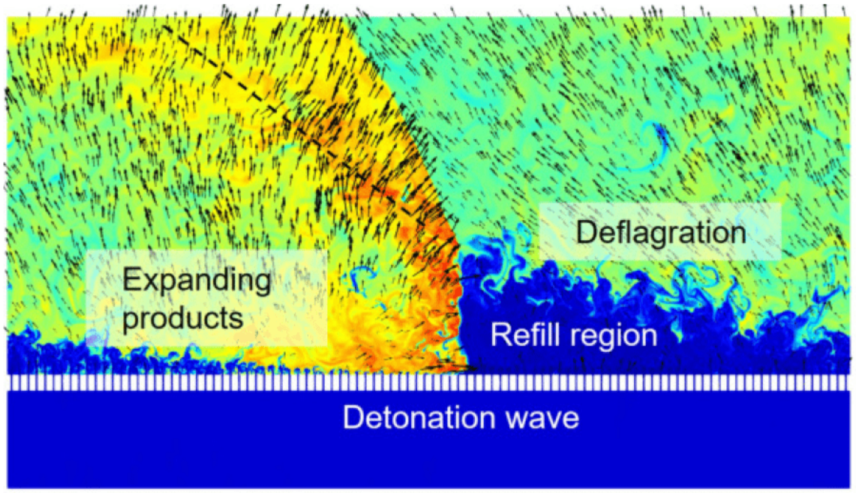

Figure 1: RDC 2D temperature distribution, velocity vector field, with indication of typical flow field features [14]

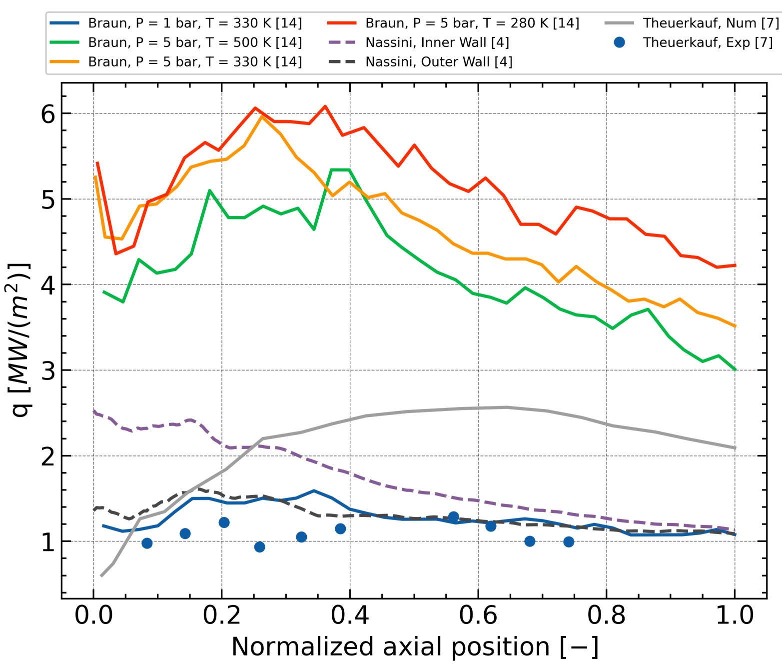

Figure 2: Comparison of heat flux profiles identified in literature

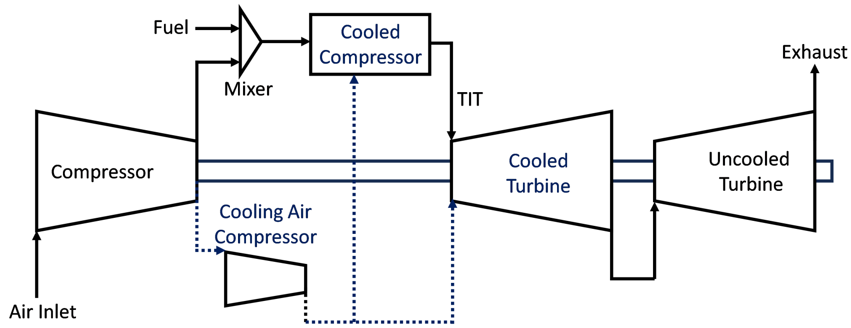

Figure 3: Gas turbine with RDC combustor and high pressure turbine cooling components layout, adapted from [16]

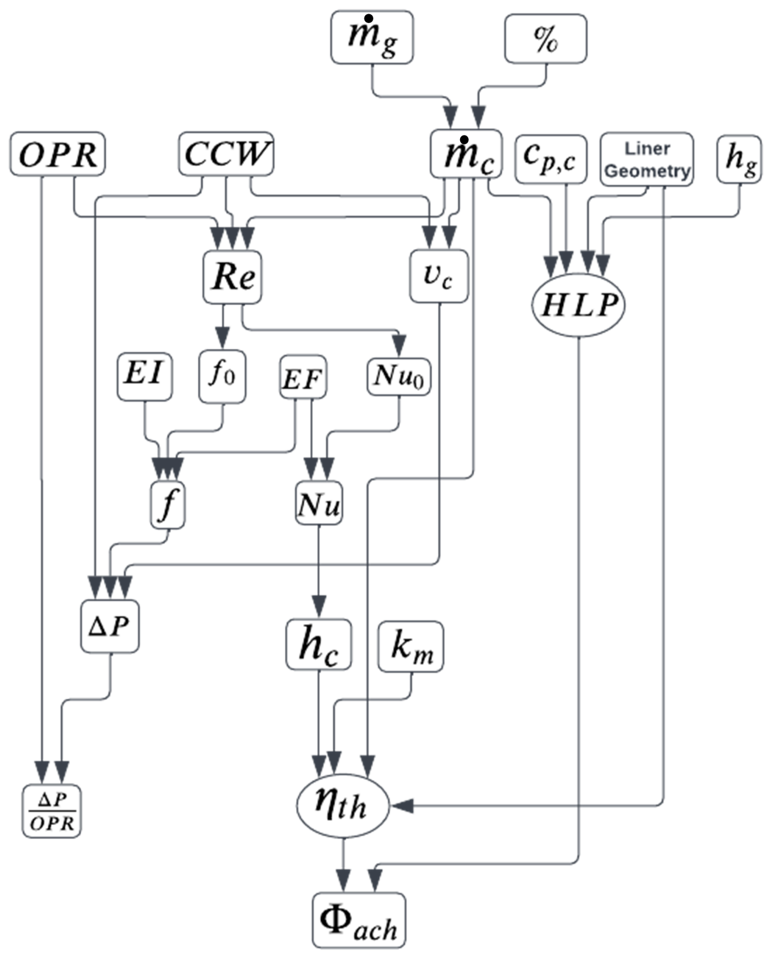

Figure 4: Calculation procedure for definition of achievable cooling effectiveness

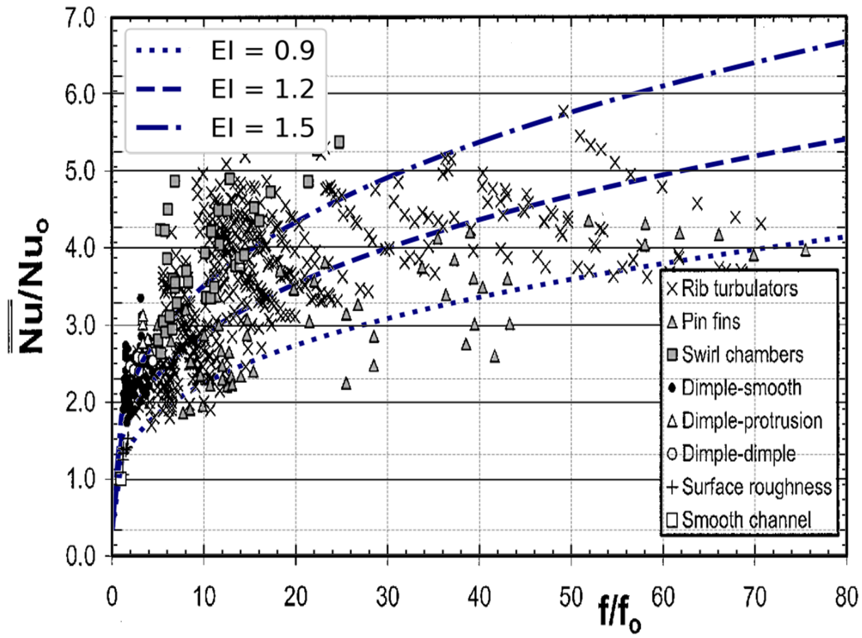

Figure 5: Adapted from Ligrani et al. [23], visualization of selected performance level *EI*

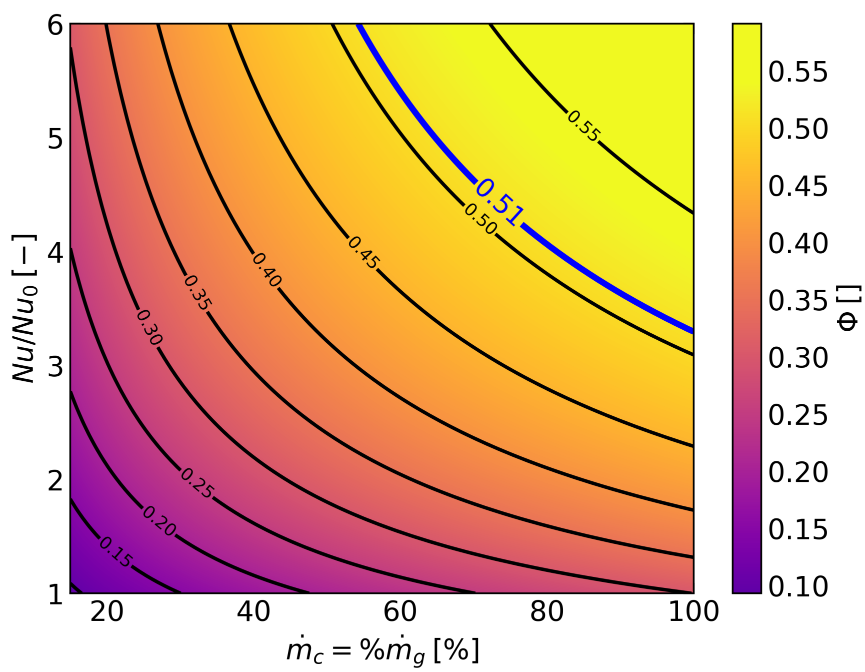

Figure 6: Achievable cooling effectiveness

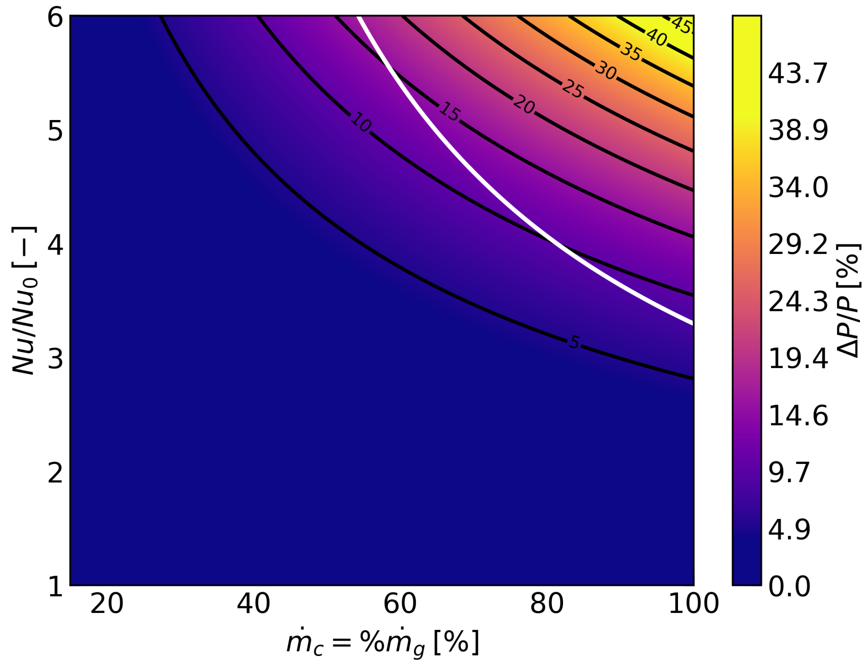

Figure 7: Pressure losses associated with a prescribed value of achievable cooling effectiveness. EI = 1.5

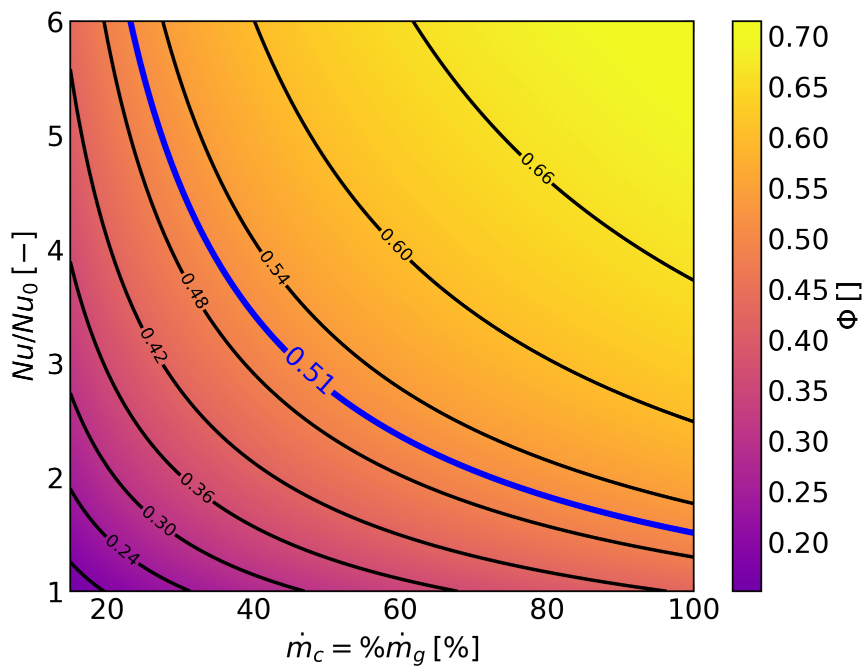

Figure 8: achievable cooling effectiveness with use of TBC

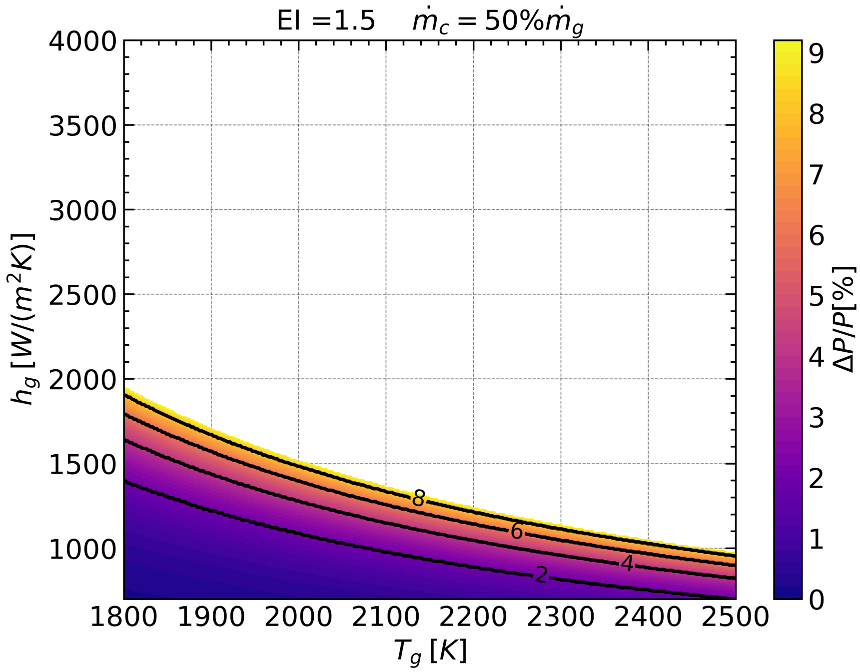

Figure 9: Pressure losses associated with different thermal loads

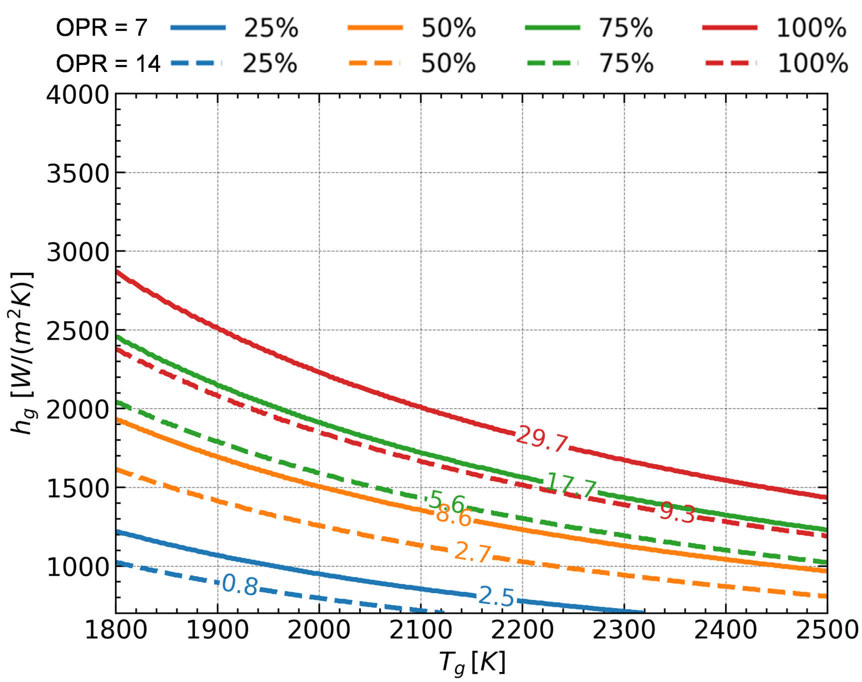

Figure 10: Pressure losses associated with different thermal loads, OPR = 7

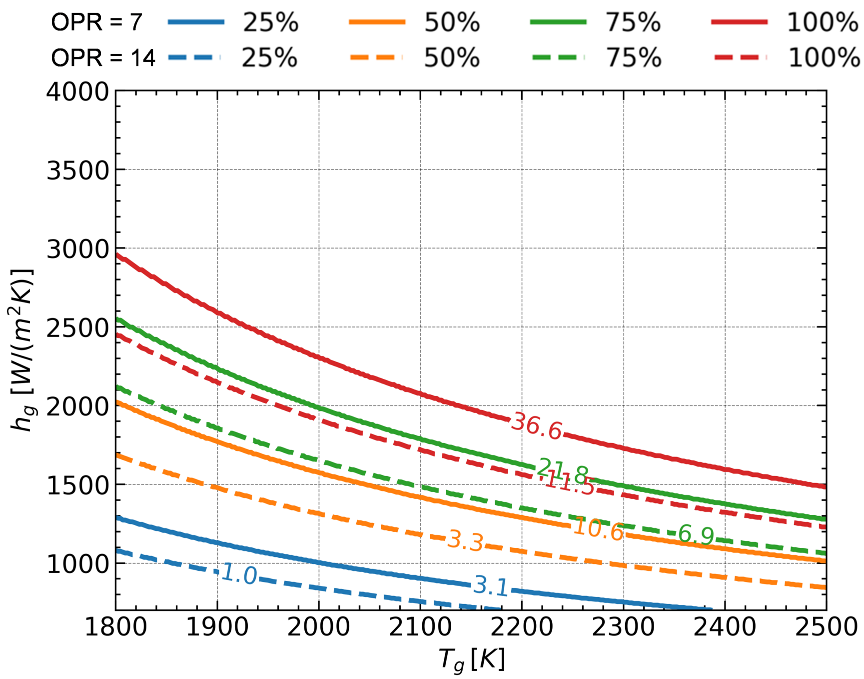

Figure 11: Pressure losses associated with different thermal loads, OPR = 7, upscaled engine

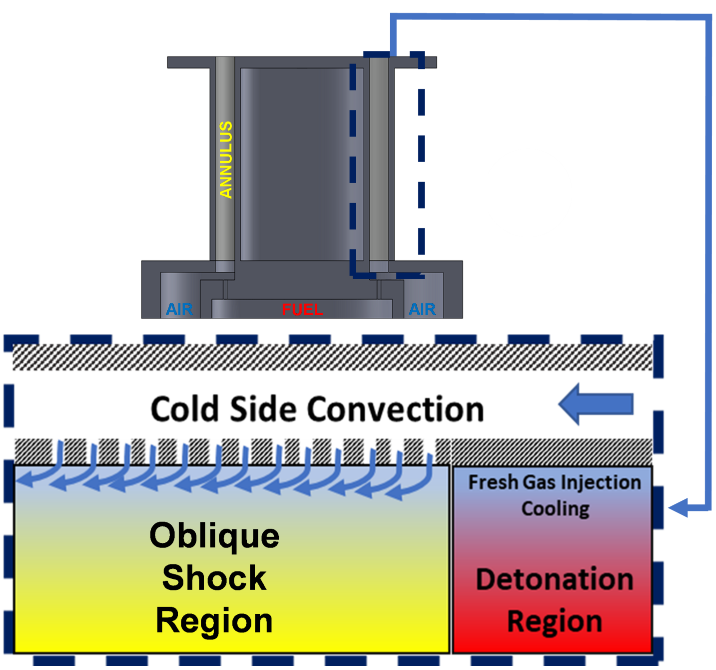

Figure 12: Reference RDC, adapted from [15], Conceptual description of cooling scheme for RDC.

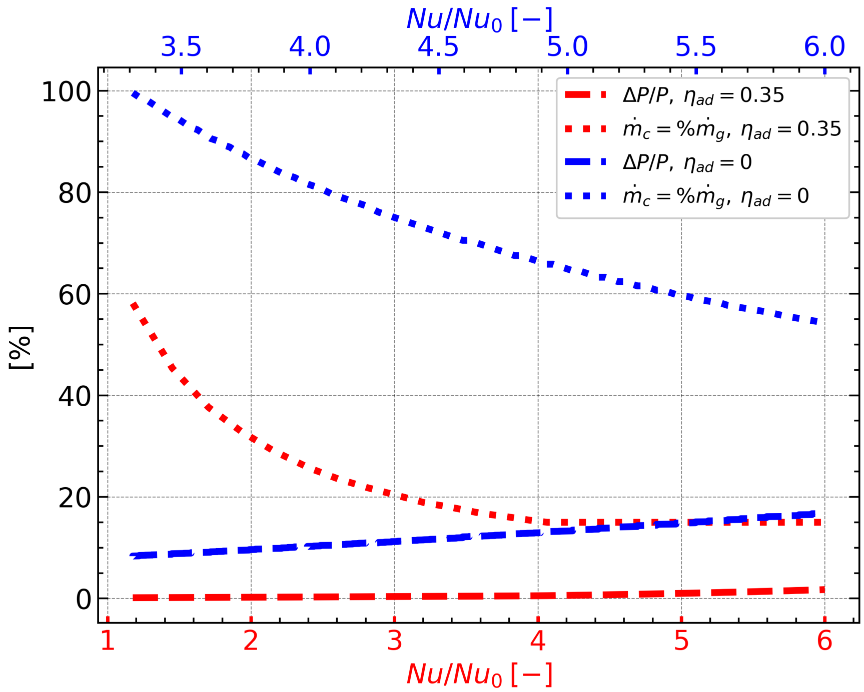

Figure 13: Effect of film cooling with $\eta_{ad} = 0.35$ on cooling requirements relative to baseline scenario

HORIZON 2020